Axial Bonding in Alkylcobalamins: DFT Analysis of the Inverse Versus Normal Trans Influence†

Jadwiga Kuta,‡ Jochen Wuerges,§ Lucio Randaccio,§ and Pawel M. Kozlowski*,‡

Department of Chemistry, University of Louisville, Louisville, Kentucky 40292, and Centre of Excellence in Biocrystallography, Department of Chemical Sciences, University of Trieste, Via L. Giorgieri 1, 34127 Trieste, Italy

Received: February 15, 2009; Revised Manuscript Received: June 1, 2009

Density functional theory has been applied to study the origin of the inverse and normal trans influence in alkylcobalamins. In order to cover the X-ray structural data available for alkylcobalamins with a variety of axial substituents, geometries of 28 related corrin-containing models have been optimized and analyzed. The BP86/6-31G(d) level of theory was applied which showed good reliability in reproducing the axial bond lengths. Comparison of experimental and calculated data allowed to conclude that the inverse trans influence is not a general feature of cobalamins, as it appeared from the experimental data analysis alone. Inverse trans influence is observed for the series of R groups with increasing bulk and electron donating ability. For the series of R groups having similar medium bulk, but differing significantly in the electron donating ability, normal trans influence was found. Finally, it was determined, that the axial bond lengths correlate well but differently in the two series of R groups with the orbital energies of the six molecular orbitals essential in axial interligand bonding.

1. Introduction

The B_{12} cofactors containing a unique Co−C σ bond belong to a class of octahedral Co(III) complexes, generally referred to as cobalamins, in which the metal center is coordinated in the equatorial position by the four corrin nitrogen atoms and in one axial position (lower face) by the 5,6-dimethylbenzimidazole (DBI) of the nucleotide side chain connected to the corrin macrocycle (Figure 1). In B_{12}-dependent enzymes, the other axial position (upper face) is occupied either by a methyl group in methylcobalamin (MeCbl) or by a 5′-deoxyadenosyl group in adenosylcobalamin (AdoCbl or coenzyme B_{12}).[1−13] Alkylcobalamins in which the upper axial ligand has structurally been modified are the subject of the active research,[13,14] particularly in context of the biologically important enzymes that use B_{12} cofactors to catalyze a variety of chemical reactions. Among different experimental techniques applied to study these complex systems, the X-ray structure determination is considered as one of the most important. This is primarily due to the fact that over the past few years the X-ray crystallographic analysis of cobalamins has been moved to a different level of reliability because of the use of the high-brilliance synchrotron radiation and improved data collection detectors.[12,14]

These advances in X-ray crystallography provide the possibility to study accurately geometrical features of cobalamins, such as those of equatorial ligands and, more importantly, of the axial fragments which are involved in the binding to proteins and in the fragmentation during enzymatic catalysis.[10,12,13] Precisely, what factors influence the lengths and strengths of the axial bonds are important from the enzymatic catalysis point of view since in all enzymatic reactions the Co−C bond is cleaved, either homolytically[15] or formally heterolytically,[16] while the Co−N_{ax} bond is either broken or elongated, depending on the specific enzymatic reaction. On the basis of the X-ray data, correlations between the axial bond lengths have been established for certain types of cobalamins. Analysis of the

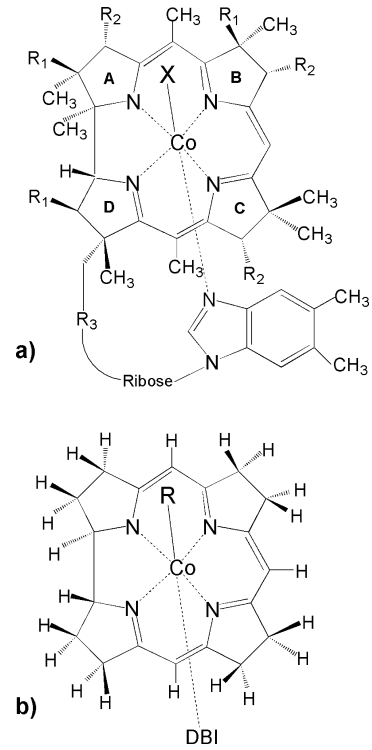

Figure 1. Molecular structure of (a) cobalamin (Cbl) where, in the biologically active forms, R is CH_3 in methylcobalamin (MeCbl) or 5′-deoxyadenosyl in adenosylcobalamin (AdoCbl) ($R_1 = CH_2CONH_2$, $R_2 = CH_2CH_2CONH_2$, $R_3 = (CH_2)_2CONHCH_2CH(CH_3)OPO_3-$) and of a (b) simplified model used in the calculations, where R is the alkyl substituent on the upper face of the corrin ring.

† Part of the "Walter Thiel Festschrift".

* To whom correspondence should be addressed. Phone: +1 502 852-6609. Fax: +1 502 852-8149. E-mail: pawel@louisville.edu.
‡ University of Louisville.
§ University of Trieste.

10.1021/jp901397p CCC: $40.75
Published on Web 07/17/2009

available structural data for models of cobalamins with different upper (or β side) axial substituents (R, Co−C bonded group) revealed that elongation of the Co−R bond either shortens (normal trans influence) or lengthens (inverse trans influence) the Co−N_{ax} bond.[17−21] The plot of the experimental Co−R versus Co−N_{ax} distances for alkylcobalamins shows a linear correlation with positive slope, thus pointing to their characteristic feature known as the inverse trans influence.

Among computational studies dealing with models of B_{12} cofactors,[19,21−56] several focused specifically on analysis of the origin of this intriguing structural behavior. Analyzing models with different α and β axial groups, Jensen et al.[55] found that, as the size of the alkyl group increases, the Co−C bond length also increases (steric cis influence). It was accompanied by not very large distortions of the corrin ring but by significant changes in the Co−N_{ax} distance (steric trans influence). Overall, they concluded that steric and electronic effects are connected and cannot be easily separated. Randaccio et al.[21] also emphasized importance of both electronic and steric effects on axial bond lengths. They have noticed that increases in σ donation from the axial group are reflected by the decrease of the positive charge on cobalt, thus causing elongation of the axial bond lengths (electronic cis and trans influence). If the bulk increases, axial bonds elongate (steric cis and trans influence), which in turn leads to more positive charge on cobalt. Therefore, both effects need to be taken into account. Hansen et al.[42] even attempted to separate steric and electronic factors in several cobaloximes by fixing Co−C and Co−N_{ax} distances and forcing the equatorial ligand to remain planar. They determined that overlap population, being their measure of the electronic effect, is not significantly different in models under consideration (methyl, isopropyl, and adenosyl were used as alkyl groups); therefore, bulk seemed to dominate over the electronic effect.

The earlier study of Bürgi et al.[19] needs to be emphasized in which an extensive analysis of a series of model complexes (cobaloximes) was carried out at a simple Hückel level of theory to explain the inverse trans influence. It was determined that the origin of the inverse trans influence lies in an unusual combination of ligands participating in axial bonding, that is, a strong σ donor (alkyl group) and a poor σ/π donor (axial base); σ donation is strong enough to reverse the expected order of the Co−C and Co−N_{ax} bond lengths based on covalent radii, making the Co−C bond stronger than that of Co−N_{ax}. Changes in R should therefore influence both the Co−C and the Co−N_{ax} distances, while replacement of DBI by a different axial base does not have any significant influence on the Co−C bond length. Indeed, resonance Raman spectra of alkylcobalamins[57,58] exhibit insensitivity of the Co−C stretching frequency with respect to the axial base displacement.

More recently, Kozlowski and co-workers applied density functional theory (DFT) to the analysis of structural and electronic properties of alkylcobalamins[45,51] in order to gain further insight into inverse trans influence at a molecular level. The aim of the present study is to continue this line of research and to provide a systematic analysis of the observed correlations, where both electronic and steric effects in the alkyl group will be taken into consideration in order to understand which factors are responsible for the origin of the inverse versus normal trans influence in alkylcobalamins.

2. Experimental and Computational Details

2.1. Experimental Data for Alkylcobalamins. Available X-ray structural data for alkylcobalamins comprise a variety of axial substituents differing in size and electronic properties.[20,33,59−64] The experimental coordination distances are summarized in Table 1 as well as in Table S1 (Supporting Information), while a plot of the experimental Co−C versus Co−N_{ax} distances is shown in Figure 2 (upper panel).

TABLE 1: Experimental Coordination Distances (Å) in Alkylcobalamins with Estimated Standard Deviations in Parentheses

R	Co−C	Co−N_{DBI}	Co−$N(av)_{short}$	Co−$N(av)_{long}$	ref
CN	1.858(12)	2.011(10)	1.875(8)	1.912(8)	59
CN(KCl)	1.868(8)	2.029(6)	1.880(5)	1.905(5)	60
CN(LiCl)	1.886(4)	2.041(3)	1.882(3)	1.916(3)	60
CF_3	1.878(10)	2.047(10)	1.894(9)	1.919(10)	20
CH=CH_2	1.911(7)	2.165(6)	1.880(5)	1.914(5)	61
CHF_2	1.949(8)	2.187(7)	1.890(7)	1.901(7)	62
cis-CH=CHCl	1.951(7)	2.144(5)	1.894(5)	1.915(5)	61
Adeninylpropyl	1.959(10)	2.212(8)	1.852(7)	1.886(7)	63
CH_3	1.979(4)	2.162(4)	1.876(4)	1.920(4)	60
Ado	2.033(4)	2.237(3)	1.873(3)	1.915(3)	33
i-Amyl	2.044(3)	2.277(2)	1.879(2)	1.914(2)	64

2.2. Methods of Calculations. All calculations reported in this work were carried out using nonlocal DFT with the nonhybrid Becke-Perdew (BP86)[65,66] functional and 6-31G(d) basis set with the 5d components for all atoms as implemented in the Gaussian 03 suite of programs for the electronic structure calculations.[67] This combination of functional and basis set, applied previously to study different properties of cobalamins,[22,26,52,54] appears to be the best to study models under consideration.[52,68] Previous work of Jensen and Ryde[27] as well as our work[52] proved a good performance of BP86, as compared with other functionals, to study cobalamin systems. Various basis sets were also tested[69] and, as the result, 6-31G(d) was chosen as the one providing the best balance between accuracy and computational cost. Calculations were performed on the simplified models, in which amide chains from the corrin ring were replaced with hydrogens, and with the nucleotide loop omitted, as depicted schematically in Figure 1b. Due to scarcity of data for imidazole, DBI was used as an axial base so direct comparison of calculated and experimental data can be provided. Orientation of R group and DBI with respect to corrin follows the experimental one.[20,33,59−64] In structures, for which there was more than one possible orientation of the R group, the one with the lowest energy was chosen.

3. Results and Discussion

3.1. Computational Models Used for the Structural Analysis. To perform analysis of the wide range of investigated axial bond lengths in alkylcobalamins (Table 1 and Table S1, Supporting Information), geometries of 28 related corrin-containing models have been optimized and analyzed. For each structure, frequency calculations were performed to verify that the corresponding geometry represents the stable minimum as confirmed by the real values of all vibrations. All relevant optimized distances are summarized in Table 2 and Table S2 (Supporting Information) and ordered according to the increasing Co−C bond lengths. Structures selected for the analysis cover a large variety of the axial R ligands (Figure 1) in terms of size and electronic properties, thus including models for which experimental data is not available for analysis of steric and electronic effects. At this point, it is worth it to mention that generally steric trans effect is understood as the structural changes in corrin ring caused by the size of one axial ligand, which destabilizes trans axial bond length. Rather moderate changes in dihedral angles of the equatorial moiety, as defined

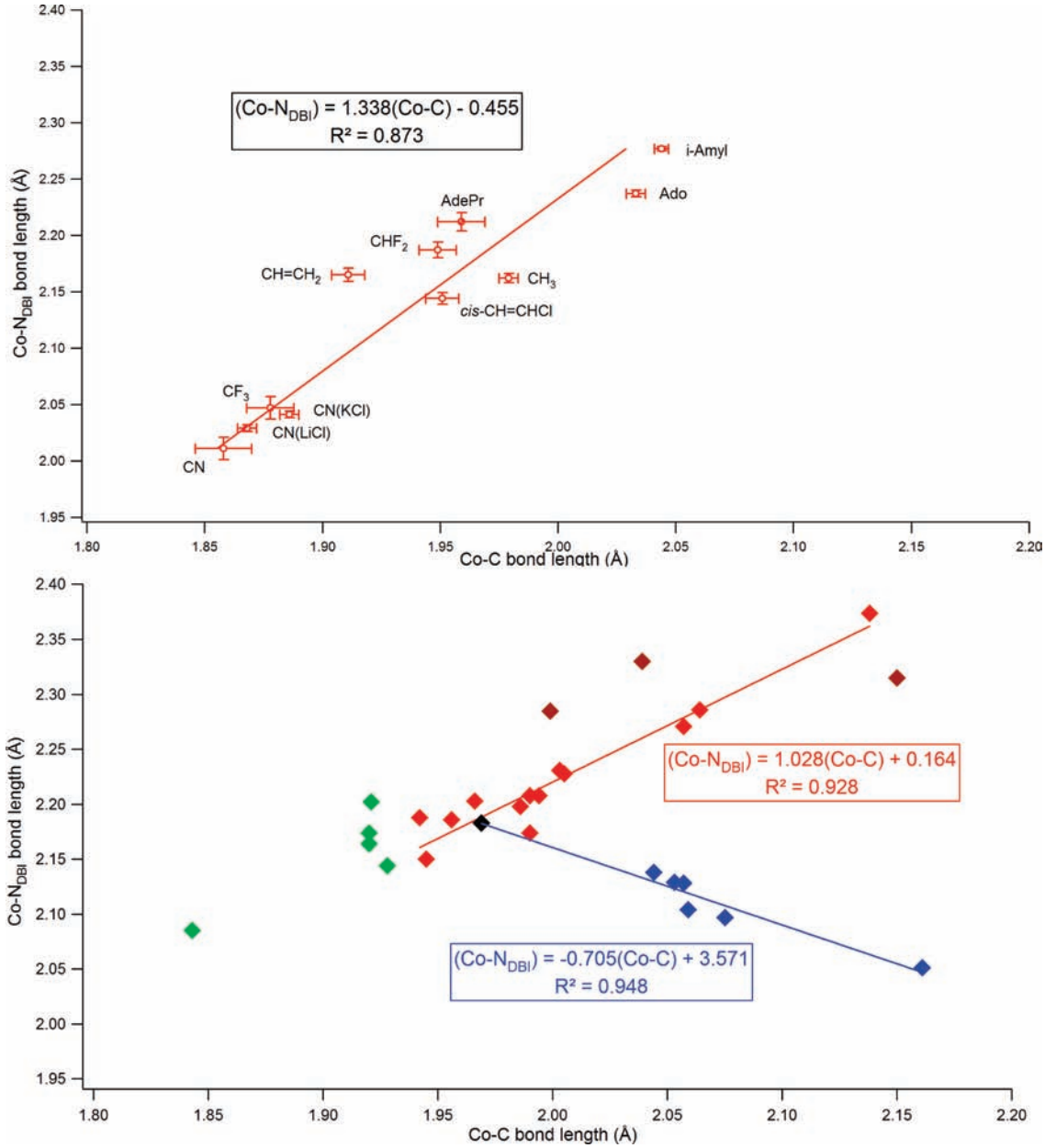

Figure 2. Upper panel: plot of experimental Co−N_{DBI} vs Co−C axial bond lengths in selected cobalamins. Lower panel: plot of calculated Co−N_{DBI} vs Co−C bond lengths grouped in several sets. Green color indicates substituents involving C hybridization different than sp^3; red indicates alkyl and fluoroalkyl substituents; blue indicates substituents with moderate bulk and different electron withdrawing ability, and maroon indicates substituents excluded from correlations. Methyl indicated in black is included in both red and blue group.

by Jensen et al.,[55,56] were observed for different alkyl groups (Table S3, Supporting Information), but an attempt to numerically correlate those changes with the Co−N_{ax} bond length has not been successful. From now on, we will refer to cis and trans steric effect as the change in the axial bond length caused by the modification on the same side or opposite side of the corrin ring, respectively.

To directly compare calculated results with experimental data, seven structures were chosen,[33,60−62,64] for which estimated standard deviations are smaller than 0.01 Å. A comparison of the axial and equatorial bond lengths for selected structures is compiled in Table 3. In order to illustrate the overall performance of the BP86/6-31G(d) level of theory, experimental axial bond lengths were plotted against the calculated axial bond lengths (Figure 3) with intercept set to zero. The slope of the linear regression is close to 1 for both Co−C and Co−N_{ax} bond lengths, which indicates good accuracy of the applied method. R^2 value for the Co−C is 0.876, which indicates fairly good fit, but R^2 value for the Co−N_{ax} is 0.787, indicating the tendency of the applied BP86/6-31G(d) level of theory to reproduce the Co−N_{ax} bond lengths more poorly for the truncated models. This most likely reflects the fact that the Co−N_{ax} bond is much weaker, about 4 times weaker than Co−C, and the corresponding energy curve for the bond stretch is rather shallow.[45,50] Furthermore, structural simplifications as well as omission of solid state effects,[54] additionally, play part in poorer reproduction of the Co−N_{ax} bond lengths.

It would have been useful to compare experimental and calculated axial distances for more bulky R groups, such as Et, i-Prop, and t-But, as well as for strongly electron-withdrawing groups, such as $C(CN)_3$. Unfortunately, no experimental data for cobalamins having the latter R groups are available. However, good linear relationships have been found when the experimental axial Co−N_{ax} and Co-R distances in cobalamins

TABLE 2: DFT BP86/6-31g(d) 5d Optimized Coordination Distances (Å) in Cobalamins[a]

alkyl group	Co−C	Co−N_{DBI}	Co−N(av)$_{short}$	Co−N(av)$_{long}$
CN[a]	1.843	2.085	1.880	1.938
cis-CH=CHCl[a]	1.920	2.164	1.868	1.934
trans-CH=CHCl[a]	1.920	2.174	1.872	1.932
CH=CH_2[a]	1.921	2.202	1.872	1.930
CH=CCl_2[a]	1.928	2.144	1.870	1.935
CHF_2[b]	1.942	2.188	1.871	1.931
CF_3[b]	1.945	2.150	1.876	1.930
CH_2F[b]	1.956	2.186	1.869	1.930
CF_2CF_3[b]	1.966	2.203	1.877	1.929
CH_3[c]	1.969	2.183	1.866	1.930
CH_2CHF_2[b]	1.986	2.198	1.870	1.930
CH_2CF_3[b]	1.990	2.174	1.870	1.934
CH_2CH_2F[b]	1.990	2.208	1.868	1.929
Ado[b]	1.994	2.208	1.870	1.926
CH_2OCH_3[d]	1.999	2.285	1.864	1.929
CH_2CH_3[b]	2.003	2.231	1.866	1.928
$CH_2CH_2CH(CH_3)_2$ (i-Amyl)[b]	2.005	2.228	1.866	1.925
CH_2NH_2[d]	2.039	2.330	1.862	1.925
$CCl_2(NO_2)$[e]	2.044	2.138	1.878	1.932
CBr_3[e]	2.053	2.129	1.876	1.930
CCl_3[e]	2.057	2.128	1.876	1.929
$CH(CH_3)_2$ (i-Prop)[b]	2.057	2.271	1.864	1.922
$CCl_2(CN)$[e]	2.059	2.104	1.880	1.930
$CF(CF_3)_2$[b]	2.064	2.286	1.874	1.938
$CCl(CN)_2$[e]	2.075	2.097	1.880	1.931
$C(CH_3)_3$ (t-But)[b]	2.138	2.374	1.864	1.925
$C(CN)_3$[e]	2.161	2.051	1.880	1.933
$C(CF_3)_3$[d]	2.315	2.150	1.878	1.935

[a] Substituents involving C hybridization different than sp^3 corresponding to green group on Figure 2. [b] Alkyl and fluoroalkyl substituents corresponding to red group on Figure 2. [c] Methyl group indicated in black on Figure 2 included in both red and blue group. [d] Substituents excluded from correlations on Figure 2 corresponding to maroon group. [e] Substituents with moderate bulk and different electron withdrawing ability corresponding to blue group on Figure 2.

are compared with the corresponding experimental distances in the simple model alkylcobaloximes $RCo(DH)_2L$ [R = alkyl group, DH = monoanion of dimethylglyoxime, L = neutral base].[14] Particularly, regressions with $R^2 = 0.95$ for the Co−X distances and $R^2 = 0.948$ for the Co−N_{ax} distances were found. Since Et, i-Prop, and adamantyl cobaloximes have been structurally characterized,[70] it is of interest to compare the calculated axial distances in cobalamins with the experimental values for the corresponding cobaloximes, $RCo(DH)_2Me_3Bzm$ (DH = monoanion of dimethylglyoxime, Me_3Bzm = 1,5,6-trimethylbezimidazole, R = Me, CH_3OCH_2, Et, i-Prop, adamantyl). Adamantyl should be a fair approximation of the t-But group. Good regressions were obtained as shown in Figure S1 (Supporting Information) with relative slopes and R^2. Such a comparison indirectly implies that the linear correlation between calculated and experimental axial distances in cobalamins should hold also for the more bulky R groups.

Lower panel of Figure 2 shows the plot of calculated Co−N_{DBI} distances against calculated Co−C distances, given in Table 2. Closer inspection of the variety of theoretical data displayed in Figure 2 shows that different alkyl R groups influence correlations between axial bond lengths in different ways, depending on their properties. The simplest way to describe the influence of R on DBI, and thus changes in the axial bond lengths, would be in terms of the bulk of R and with its electronic properties. Although the concept of steric and electronic properties of the axial ligand is relatively easy to envision conceptually, in practice it is difficult to parametrize and quantify, mostly because of scarcity of experimental data.

Again, in cobaloximes quantitative rationalization of the experimental axial distances has been achived in terms of electronic and steric properties of the alkyl group. Principal component analysis (PCA)[71] for those systems gave a three component model which allowed for the interpretation of kinetic, spectroscopic, structural, and thermodynamic data of alkylcobaloximes by using the equation

$$Q_L = a_0 + a_1 t_1 + a_2 t_2 + a_3 t_3 \quad (1)$$

where Q_L is the analyzed property of the series with a given L ligand and different R groups and a_i represents the contribution of the t_i parameter; t_1 values increase with the increasing σ electron-donating ability of groups substituting the H methyl atoms; t_2 values follow the increase in bulk of R, while t_3 is interpreted as a measure of the angular distortion at C connected to Co. Application of eq 1 to calculate axial distances in alkylcobalamins, for which t_1, t_2, and t_3 were available, worked analogously as in alkylcobaloximes (Table 4). The corresponding equations of type 1 indicated that both Co−N_{DBI} and Co−C axial distances depend on both bulk and electron donating properties of the alkyl group. The plots of distances determined by eq 1 against the corresponding ones obtained by DFT are shown in Figure 4 with good linear correlations, thus showing that PCA can be successfully used to analyze electronic and steric properties of the alkyl groups, as applied for alkylcobalamins.

The analysis of correlations on the lower panel of Figure 2 was limited essentially to the R groups with a Co−C(sp^3) bond. Thus, CN and vinyl derivatives were excluded, since the different hybridization of the α-C bonded to Co and a possible π-back-donation from metal to carbon should influence differently the Co−C bond with respect to the sp^3 hybridization (indicated in green in Table 1 and Figure 2). We observe that the remaining R ligands can be grouped into two series. One contains alkyl and fluoroalkyl ligands with significantly increasing bulk and electron σ-donating ability (from CF_3 to $C(CH_3)_3$), as suggested by the available values of t_1 and t_2 (Table 4). The

TABLE 3: Comparison of Calculated and Experimental Co−C and Co−N_{DBI} Axial Bond Lengths and Co−N Equatorial Bond Lengths (With ESD Less than 0.01 Å)

	Co−C	Co−C	Co−N_{DBI}	Co−N_{DBI}	Co−N(av)$_{short}$	Co−N(av)$_{short}$	Co−N(av)$_{long}$	Co−N(av)$_{long}$
	calc	exp	calc	exp	calc	exp	calc	exp
CN	1.843	1.886	2.085	2.041	1.880	1.882	1.938	1.916
cis-CH=CHCl	1.920	1.951	2.174	2.144	1.868	1.894	1.934	1.915
CH=CH_2	1.921	1.911	2.202	2.165	1.872	1.880	1.930	1.914
CHF_2	1.942	1.949	2.188	2.187	1.871	1.890	1.931	1.901
CH_3	1.969	1.979	2.183	2.162	1.866	1.876	1.930	1.920
Ado	1.994	2.033	2.208	2.237	1.870	1.873	1.926	1.915
i-Amyl	2.005	2.044	2.228	2.277	1.866	1.879	1.925	1.914

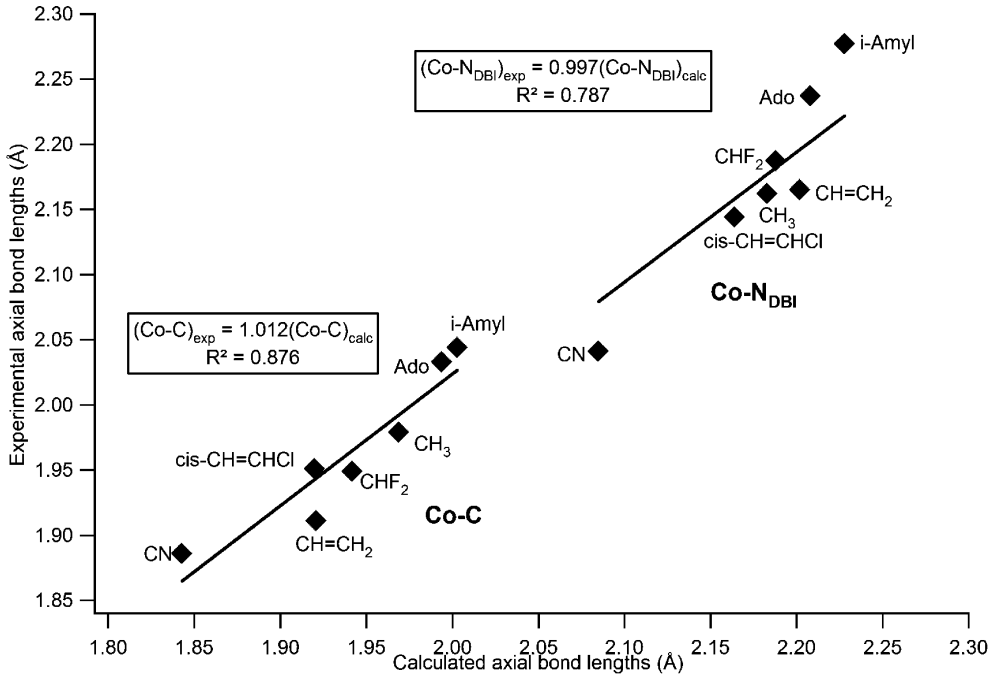

Figure 3. Comparison of calculated and experimental Co−C and Co−N_{DBI} axial bond lengths with intercept set to 0.

TABLE 4: Available t_1, t_2, and t_3 for Some Cobalamins and PCA Predicted Axial Bond Length Compared with the DFT Results (Å)

alkyl group	Co−N_{DBI} DFT	Co−C DFT	t_1	t_2	t_3	Co−N_{DBI} PCA[a]	Co−C PCA[a]
CF_3	2.150	1.945	−2.48	−0.57	−1.11	2.161	1.947
CH_3	2.183	1.969	0.10	−1.91	0.07	2.191	1.972
CH_2CF_3	2.174	1.990	−1.31	−0.20	−0.03	2.194	1.989
Ado	2.208	1.994	0.05	−1.11	−0.16	2.210	1.988
CH_2OCH_3	2.285	1.999	1.55	−1.71	−0.13	2.237	1.999
CH_2CH_3	2.231	2.003	1.10	−1.35	0.24	2.231	2.005
$CH(CH_3)_2$	2.271	2.057	2.19	0	0.10	2.293	2.056
$CF(CF_3)_2$	2.286	2.064	−1.65	3.08	−0.03	2.261	2.065
$C(CH_3)_3$	2.374	2.138	3.69	2.20	0.30	2.384	2.139

[a] The linear regressions for the Co−C and Co−N_{DBI} are (see eq 1): (Co−C) = 2.017(1) + 0.0172(8)t_1 + 0.0249(7)t_2 + 0.012(4)t_3 (Co−N_{DBI}) = 2.234(10) + 0.027(7)t_1 + 0.0234(6)t_2

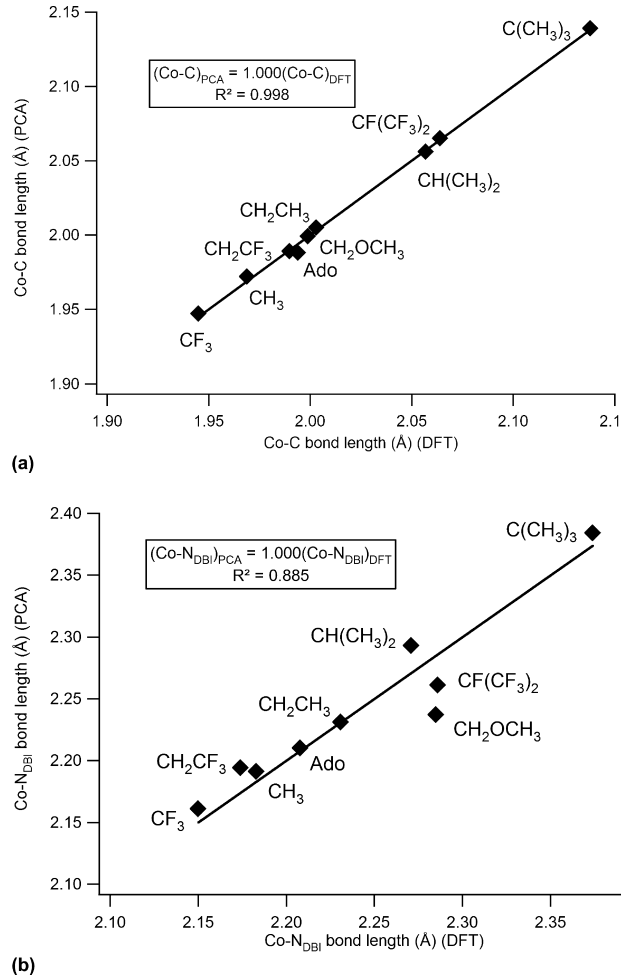

Figure 4. Comparison of (a) Co−C and (b) Co−N_{DBI} axial distances determined by DFT and PCA. Intercept was set to 0.

other series contains ligands with similar moderate bulk and very different electron withdrawing/donating ability. The two series are indicated in red and blue, respectively, in Figure 2 (lower panel). The methyl group (black) is included in both correlations. It also needs to be mentioned that the choice of the two series is rather arbitrary. The points corresponding to CH_2OCH_3, CH_2NH_2, and $C(CF_3)_3$ (maroon) were not included in the correlations as the latter should have a very large bulk and the other two are strong σ donors with a small bulk. The trends of the Co−N_{DBI} distances against the Co−C distances show very good correlations ($R^2 = 0.928$ and 0.948 for the first and second series, respectively). However, we note that they significantly differ in the electronic and steric properties of the R groups: as stressed above, the first series contains groups with both significantly different bulk and electron donating ability, whereas in the second one, the groups have fairly similar bulk and largely different electron donating ability. The red and blue lines in Figure 2 (lower panel) exemplify the inverse and normal trans influence, respectively.

By comparing experimental and calculated data (Figure 2), it can be concluded that the inverse trans influence is not a general feature of cobalamins, as it appeared from the experimental data analysis alone. Interestingly, the experimental axial distances for bulky R groups of the second series are not available. This seems to be the reason, why normal

trans influence is not observed among experimentally available data plotted in the upper panel of Figure 2, whereas it is present in the calculated data (lower panel of Figure 2).

3.2. Orbital Description of the Axial Bonding in Alkylcobalamins. PCA analysis allowed us to establish how steric and electronic properties of the alkyl groups influence axial bond lengths within the first series of analyzed R groups, which produce inverse trans influence. This is not the case for the second series, producing normal trans influence. In this case, PCA could not be applied because of a lack of availability of appropriate experimental data. In an attempt to understand the origin of the normal trans influence as compared with that of the inverse trans influence, our analysis was shifted toward Kohn−Sham molecular orbitals (MOs) and their energies that can be extracted from the DFT calculations (Figure 5 and Figures S2,S3, Supporting Information). Following the previous study,[51] six MOs are needed for the concise description of the interligand bonding. The prerequisite for the description of the axial bonding is the d_{z^2} orbital on cobalt which mixes with the p_z orbital on carbon and with the p_z orbital on the axial nitrogen (eqs 2−4):

$$\sigma_1 \approx + c_{11}\varphi[N_B(\mathrm{s}, \mathrm{p}_z)] + c_{12}\varphi[Co(\mathrm{d}_{z^2})] + c_{13}\varphi[C_R(\mathrm{s}, \mathrm{p}_z)] \quad (2)$$

$$\sigma_2 \approx - c_{21}\varphi[N_B(\mathrm{s}, \mathrm{p}_z)] + c_{22}\varphi[Co(\mathrm{d}_{z^2})] + c_{23}\varphi[C_R(\mathrm{s}, \mathrm{p}_z)] \quad (3)$$

$$\sigma_3^* \approx - c_{31}\varphi[N_B(\mathrm{s}, \mathrm{p}_z)] + c_{32}\varphi[Co(\mathrm{d}_{z^2})] - c_{33}\varphi[C_R(\mathrm{s}, \mathrm{p}_z)] \quad (4)$$

The mixing of the three atomic orbitals (AOs) leads to the σ_1 orbital being strongly bonding with respect to both cobalt and carbon, as well as cobalt and nitrogen, the σ_2 orbital being bonding with respect to cobalt and carbon, but antibonding with respect to cobalt and nitrogen, and σ_3* being antibonding with respect to both cobalt and carbon, as well as cobalt and nitrogen. This model has only semiquantitative meaning and is further complicated by the involvement of the corrin π-type orbitals, the d_{xy} orbital on cobalt, and the p_x and p_y orbitals on nitrogen (eqs 5−7):

$$\psi_1^{\pm} \approx \sigma_1 \pm \chi_1^{\pm}\{\varphi[Co(\mathrm{d}_{xy})] \pm \lambda_1\varphi[N_B(\mathrm{p}_x, \mathrm{p}_y)]\} \quad (5)$$

$$\sigma_2^{\pm} \approx \chi_2^{\pm}\varphi[\pi_{corr}] \pm \sigma_2 \quad (6)$$

$$\psi_3^{*\pm} \approx \sigma_3^* \pm \chi_3^{\pm}\{\varphi[Co(\mathrm{d}_{xy})] \pm \lambda_3\varphi[N_B(\mathrm{p}_x, \mathrm{p}_y)]\} \quad (7)$$

It was shown previously for selected cobalamins ($-CF_3$, $-CH_3$, $-CH_2NH_2$)[51] that the electron donating ability of the alkyl group is primarily responsible for elongation observed for both Co−C and Co−N_{ax} distances. Analysis of the orbital energies revealed that the electron donation induced by the R group raises energies of MOs associated with axial bonds and diminishes interligand bonding. On the basis of those results, it was concluded that an orbital analysis can provide an explanation why, for cobalamin models, inverse trans influence is observed. A similar orbital analysis is extended in the current work and directed toward a more thorough understanding of both inverse and normal trans influence.

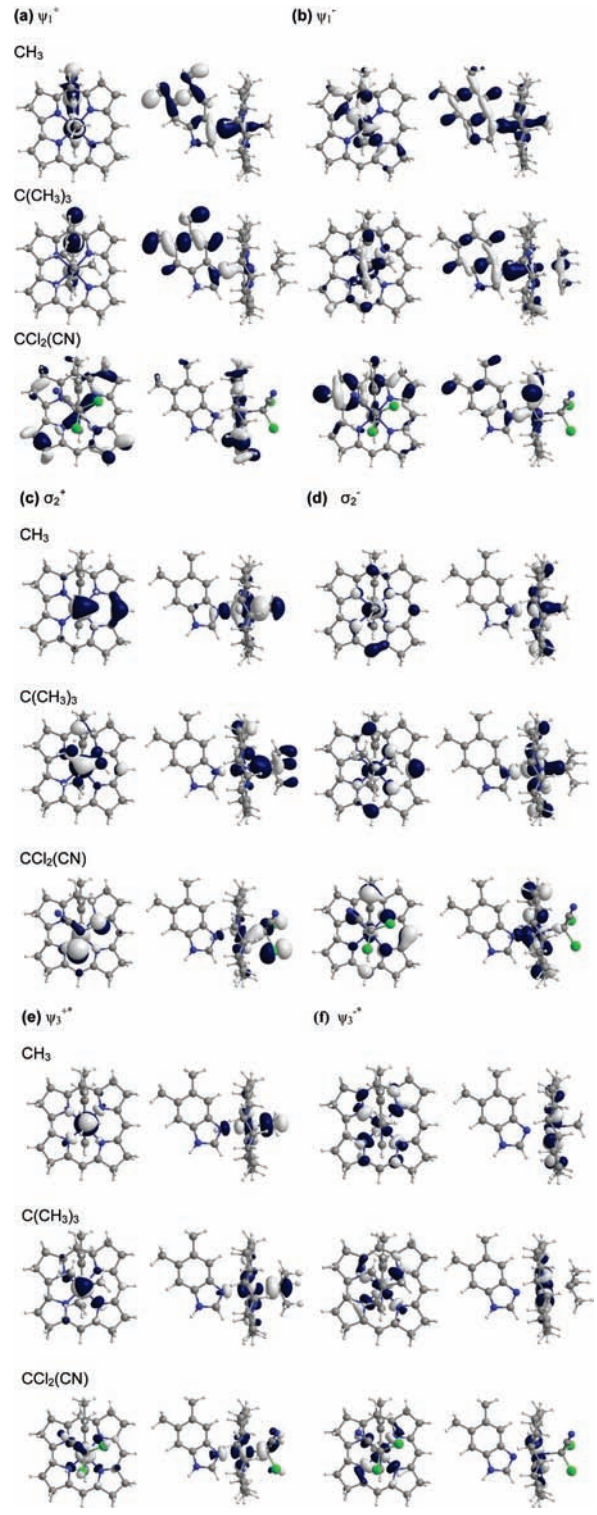

Figure 5. Pictures of six molecular orbitals essential in interligand bonding for three representative models, involving CH_3 (Set 1), $C(CH_3)_3$ (Set 1), and $CCl_2(CN)$ (Set 2) as the axial substituents.

For further analysis of relationships between the axial bond lengths, two sets with different properties of the alkyl substituents were chosen: Set 1 with alkyls belonging to the first group ($-CH_3$, $-CH_2CH_3$, $-CH(CH_3)_2$, $-C(CH_3)_3$) and Set 2 with alkyls belonging to the second group ($-C(CN)_3$, $-CCl(CN)_2$, $-CCl_2(CN)$, $-CCl_3$).

Orbital energy level diagrams for the two sets are shown in Figure S2 (Supporting Information), sorted according to the increasing Co−C bond length within each set. Comparison of

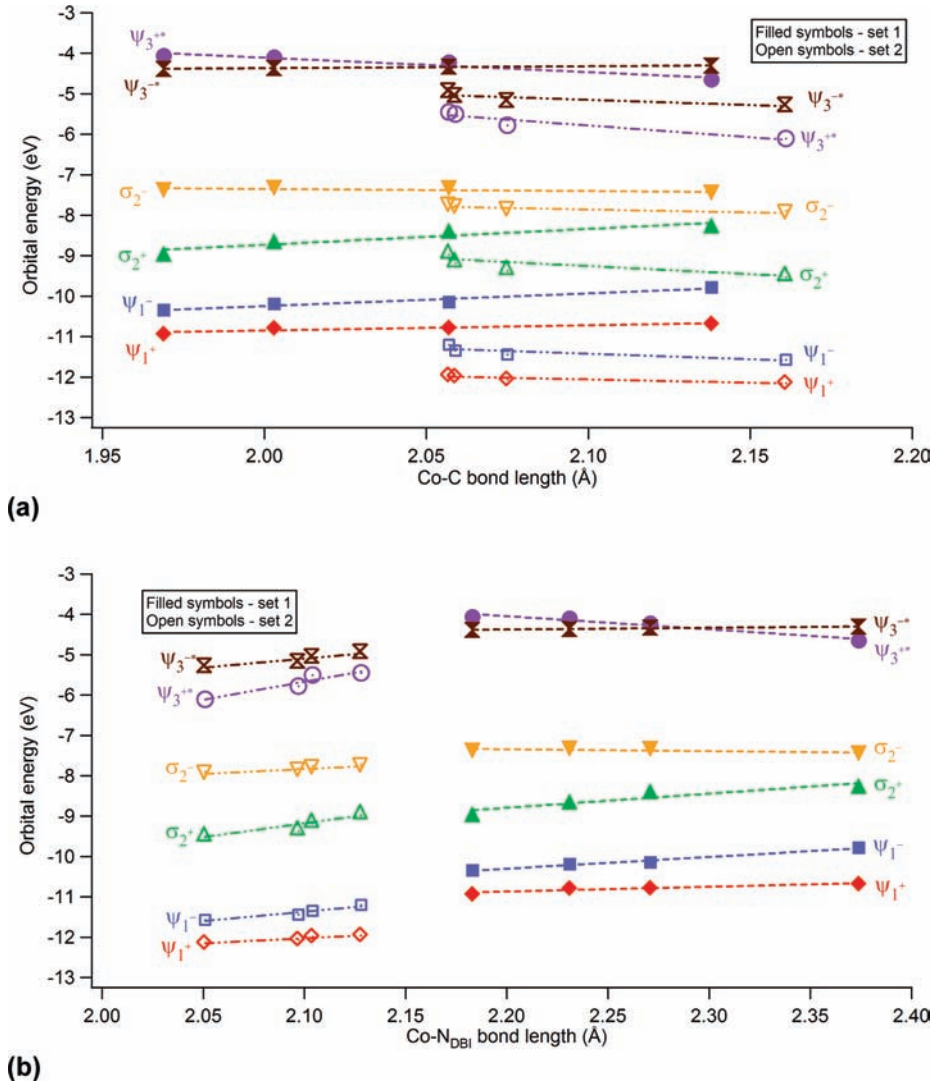

Figure 6. Comparison of orbital energy correlations for Set 1 (increasing bulk and increasing electron donating ability) and Set 2 (medium bulk and increasing electron donating ability) versus (a) Co−C bond length and (b) Co−N_{DBI} bond length.

the orbital energies for the six molecular orbitals essential in the interligand bonding reveals that, for Set 1, orbital energies of Ψ_1^+, Ψ_1^-, σ_2^+, σ_2^-, and $\Psi_3{}^{*-}$ increase with increasing Co−C bond length, while orbital energies of $\Psi_3{}^{*+}$ decrease. Correspondingly, the inverse trans influence is observed. For Set 2, orbital energies are decreasing as the Co−C bond length increases. Correspondingly, the normal trans influence is observed.

3.3. Orbital Analysis of the Inverse and Normal Trans Influence. To elucidate the inverse and normal trans influence and thus to some degree quantify steric and electronic effects for Set 2, changes of the orbital energies essential in interligand bonding (Table S4, Supporting Information) were plotted as a function of the axial bond lengths for the two chosen sets (Figure 6). Those two sets cover different ranges of the Co−C bond lengths and their bulk and electronic properties affect orbital energies in different ways. In most cases, linear correlations with good R^2 values were obtained, but in a few cases no significant variation of the orbital energy with the axial distances was noted (Table 5 and 6).

For the Co−N_{ax} distances, the slopes of the orbital energy against distances in both sets are all positive (with the exception of the $\Psi_3{}^{*+}$ for Set 1); correspondingly, the Co−N_{ax} distances increase with the increase of the electronic trans influence of R and are not affected by the bulk of R. For the Co−C distances, the slopes in Set 1 are positive and correspond to the increase of the Co−C distance with the electronic influence and with bulk of R (again, with the exception of the $\Psi_3{}^{*+}$). In Set 2, the slopes are negative; correspondingly, the Co−C distances increase with the decrease in the electronic influence. Those results clearly show that the change in the orbital energy influences the length of the axial Co−N and Co−C distances differently for Set 2 with respect to Set 1, as shown in Figure 2.

In Set 1, not only is the electron donating ability increasing ($-CH_3 \rightarrow -CH_2CH_3 \rightarrow -CH(CH_3)_2 \rightarrow -C(CH_3)_3$), but also the bulk of the R group needs to be taken into consideration,

TABLE 5: Linear Fit Parameters for the Orbital Energy Versus Co−C Bond Length Correlations Where Numerical Values for Correlations, in Which R^2 Was Smaller than 0.5, Were Not Shown

	set 1			set 2		
orbital	slope	intercept	R^2	slope	intercept	R^2
Ψ_1^+	1.284	−13.418	0.848	−1.603	−8.694	0.876
Ψ_1^-	2.598	−15.442	0.952	−2.677	−5.801	0.720
σ_2^+	3.932	−6.593	0.878	−3.918	−1.035	0.641
σ_2^-				−1.445	−4.825	0.808
$\Psi_3{}^{*+}$	−3.540	2.971	0.931	−5.814	6.429	0.892
$\Psi_3{}^{*-}$	0.481	−5.333	0.943	−2.596	0.303	0.718

TABLE 6: Linear Fit Parameters for the Orbital Energy Versus Co−N_{DBI} Bond Length Correlations Where Numerical Values for Correlations, in Which R^2 Was Smaller than 0.5, Were Not Shown

	set 1			set 2		
orbital	slope	intercept	R^2	slope	intercept	R^2
Ψ_1^+	1.188	−13.486	0.882	2.537	−17.355	0.935
Ψ_1^-	2.398	−15.568	0.986	4.646	−21.124	0.925
σ_2^+	3.514	−16.524	0.852	6.904	−23.678	0.847
σ_2^-				2.360	−12.787	0.918
$\Psi_3{}^{*+}$	3.238	3.076	0.947	8.981	−24.525	0.907
$\Psi_3{}^{*-}$	0.426	−5.316	0.900	4.450	−14.441	0.900

which is in fact the reason why the slope for the $\Psi_3{}^{*+}$ correlation is negative. The $\Psi_3{}^{*+}$ orbital has strong antibonding character (eq 4 and 7), both with respect to cobalt and carbon, as well as with respect to cobalt and nitrogen. Increasing size of the R group causes steric repulsion and therefore weakens interactions between the d_z^2 orbital on cobalt with the p_z orbital on carbon, and between d_z^2 orbital on cobalt and p_z orbital on the axial nitrogen, thus diminishing antibonding character of this orbital and stabilizing it, while the bulk increases. Generally, increasing bulk causes elongation of axial bond lengths (steric influence), which slightly diminishes electron donation from the alkyl substituents. Decrease in the electron donation would cause a slight lowering of orbital energies. Those results are consistent with the PCA, indicating that both steric and electronic properties of the R group influence axial bond lengths.

A closer look at the correlations for Set 2 allows one to notice that the orbital energies are stabilized as electron donation from the alkyl group decreases ($-CCl_3 \rightarrow -CCl_2(CN) \rightarrow -CCl(CN)_2 \rightarrow -C(CN)_3$). This leads to a bigger positive charge on cobalt and a stronger attraction of the negatively charged axial base but a repulsion of the alkyl group. Therefore, the Co−N_{ax} bond length decreases as the Co−C bond length increases, which overall produces normal trans influence. It can be thus concluded that for Set 2 with no significant change in bulk, mostly electronic properties of the R groups are responsible for the occurrence of the normal trans influence.

4. Summary and Conclusions

The main goal of the present work was the analysis of the nature of the inverse and normal trans influence in alkylcobalamins. First, the applied BP86/6-31G(d) level of theory proved to be reliable in reproducing essential geometrical features of the models used in analysis, as compared with the available experimental data. Comparison of experimental and calculated data allowed for the conclusion that the inverse trans influence is not a general feature of cobalamins, as it appeared from the experimental data analysis alone. For the series of R groups having similar bulk, but significantly large difference in the electron donating ability, normal trans influence was found. Interestingly, the experimental axial distances for the latter R groups are not available. This appears to be the reason why normal trans influence is not observed among experimentally available data. Inverse trans influence is observed for substituents with increasing bulk and electron donating ability. An attempt was made to answer the question why, for systems with certain groups of the axial substituents inverse, while for others normal trans influence is observed, which could not be explained on the basis of the limited experimental data alone. After analyzing a variety of the axial substituents in the computational models, it was determined that the axial bond lengths correlate well but differently in the two series of R groups, with the orbital energies of the six molecular orbitals essential in interligand bonding. Those correlations, as well as PCA for the group of substituents with increasing bulk and increasing electron donating ability, allowed for the establishment that both electronic and steric properties of the R group influence axial bond lengths, while for the group with similar medium bulk, but different electron donating ability, mostly electronic effect is responsible for the changes in the axial bond lengths.

Supporting Information Available: Complete list of axial and equatorial coordination distances for experimental and calculated data, orbital energies, Cartesian coordinates of all optimized structures, orbital energy level diagrams, orbital pictures, plot comparing experimental data for cobaloximes with calculated data for cobalamins. This material is available free of charge via the Internet at http://pubs.acs.org.

References and Notes

(1) Dolphin, D. *B_{12}*; Wiley-Interscience: New York, 1982.
(2) Banerjee, R. *Chem. Biol.* **1997**, *4*, 175–186.
(3) Ludwig, M. L.; Matthews, R. G. *Annu. Rev. Biochem.* **1997**, *66*, 269–313.
(4) Kräutler, B.; Arigoni, D.; Golding, B. T. *Vitamin B_{12} and B_{12}-Proteins*; Wiley-VCH: New York, 1998.
(5) Marzilli, L. G. In *Bioinorganic Catalysis*; Reedijk, J., Bouwman, E., Eds.; Marcel Dekker: New York, 1999; pp 423−468.
(6) Banerjee, R. *Chemistry and Biochemistry of B_{12}*; John Wiley and Sons: New York, 1999.
(7) Toraya, T. *Cell. Mol. Life Sci.* **2000**, *57*, 106–127.
(8) Banerjee, R. *Biochemistry* **2001**, *40*, 6191–6198.
(9) Banerjee, R.; Ragsdale, S. W. *Annu. Rev. Biochem.* **2003**, *72*, 209–247.
(10) Banerjee, R. *Chem. Rev.* **2003**, *103*, 2083–2094.
(11) Toraya, T. *Chem. Rev.* **2003**, *103*, 2095–2127.
(12) Brown, K. L. *Chem. Rev.* **2005**, *105*, 2075–2149.
(13) Randaccio, L.; Geremia, S.; Wuerges, J. *J. Organomet. Chem.* **2007**, *692*, 1198–1215.
(14) Randaccio, L.; Geremia, S.; Nardin, G.; Wuerges, J. *Coord. Chem. Rev.* **2006**, *250*, 1332–1350.
(15) Halpern, J. *Science* **1985**, *227*, 869–875.
(16) Matthews, R. G. *Acc. Chem. Res.* **2001**, *34*, 681–689.
(17) Bresciani-Pahor, N.; Forcolin, M.; Marzilli, L. G.; Randaccio, L.; Summers, J. S.; Toscano, P. J. *Coord. Chem. Rev.* **1985**, *63*, 1–125.
(18) Randaccio, L.; Bresciani-Pahor, N.; Zangrando, E. *Chem. Soc. Rev.* **1989**, *18*, 225–250.
(19) DeRidder, D. J. A.; Zangrando, E.; Burgi, H.-B. *J. Mol. Struct.* **1996**, *374*, 63–83.
(20) Zou, X.; Brown, K. L. *Inorg. Chim. Acta* **1998**, *267*, 305–308.
(21) Randaccio, L.; Geremia, S.; Stener, M.; Toffoli, D.; Zangrando, E. *Eur. J. Inorg. Chem.* **2002**, *2002*, 93–103.
(22) Dölker, N.; Maseras, F.; Lledos, A. *J. Phys. Chem. B* **2001**, *105*, 7564–7571.
(23) Dölker, N.; Maseras, F.; Lledos, A. *J. Phys. Chem. B* **2003**, *107*, 306–315.
(24) Dölker, N.; Maseras, F.; Siegbahn, P. E. M. *Chem. Phys. Lett.* **2004**, *386*, 174–178.
(25) Dölker, N.; Morreale, A.; Maseras, F. *J. Biol. Inorg. Chem.* **2005**, *10*, 509–517.
(26) Jensen, K. P.; Ryde, U. *J. Mol. Struc. (Theochem)* **2002**, *585*, 239–255.
(27) Jensen, K. P.; Ryde, U. *J. Phys. Chem. A* **2003**, *107*, 7539–7545.
(28) Jensen, K. P.; Ryde, U. *J. Am. Chem. Soc.* **2003**, *125*, 13970–13971.
(29) Jensen, K. P.; Ryde, U. *ChemBioChem* **2003**, *4*, 413–424.
(30) Geremia, S.; Calligaris, M.; Randaccio, L. *Eur. J. Inorg. Chem.* **1999**, 981–992.
(31) Ouyang, L.; Randaccio, L.; Rulis, P.; Kurmaev, E. Z.; Moewes, A.; Ching, W. Y. *J. Mol. Struc. (Theochem)* **2003**, *622*, 221–227.
(32) Kurmaev, E. Z.; Moewes, A.; Ouyang, L.; Randaccio, L.; Rulis, P.; Ching, W. Y.; Bach, M.; Neumann, M. *Europhys. Lett.* **2003**, *62*, 582–587.
(33) Ouyang, L.; Rulis, P.; Ching, W. Y.; Nardin, G.; Randaccio, L. *Inorg. Chem.* **2004**, *43*, 1235–1241.
(34) Marques, H. M.; Brown, K. L. *J. Mol. Struc. (Theochem)* **1995**, *340*, 97–124.
(35) Brown, K. L.; Marques, H. M. *Polyhedron* **1996**, *15*, 2187–2197.
(36) Brown, K. L.; Zou, X.; Marques, H. M. *J. Mol. Struc. (Theochem)* **1998**, *453*, 209–224.

(37) Marques, H. M.; Warden, C.; Monye, M.; Shongwe, M. S.; Brown, K. L. *Inorg. Chem.* **1998**, *37*, 2578–2581.
(38) Marques, H. M.; Brown, K. L. *Coord. Chem. Rev.* **1999**, *190*−*192*, 127–153.
(39) Brown, K. L.; Marques, H. M. *J. Inorg. Biochem.* **2001**, *83*, 121–132.
(40) Marques, H. M.; Ngoma, B.; Egan, T. J.; Brown, K. L. *J. Mol. Struct.* **2001**, *561*, 71–91.
(41) Marques, H. M.; Brown, K. L. *Coord. Chem. Rev.* **2002**, *225*, 123–158.
(42) Hansen, L. M.; Paran-Kumar, N. V. P.; Marynick, D. S. *Inorg. Chem.* **1994**, *33*, 728–735.
(43) Hansen, L. M.; Derecskei-Kovacs, A.; Marynick, D. S. *J. Mol. Struc. (Theochem)* **1998**, *431*, 53–57.
(44) Andruniow, T.; Zgierski, M. Z.; Kozlowski, P. M. *Chem. Phys. Lett.* **2000**, *331*, 502–508.
(45) Andruniow, T.; Zgierski, M. Z.; Kozlowski, P. M. *J. Phys. Chem. B* **2000**, *104*, 10921–10927.
(46) Andruniow, T.; Zgierski, M. Z.; Kozlowski, P. M. *J. Am. Chem. Soc.* **2001**, *123*, 2679–2680.
(47) Andruniow, T.; Kozlowski, P. M.; Zgierski, M. Z. *J. Chem. Phys.* **2001**, *115*, 7522–7533.
(48) Andruniow, T.; Zgierski, M. Z.; Kozlowski, P. M. *J. Phys. Chem. A* **2002**, *106*, 1365–1373.
(49) Kozlowski, P. M.; Zgierski, M. Z. *J. Phys. Chem. B* **2004**, *108*, 14163–14170.
(50) Freindorf, M.; Kozlowski, P. M. *J. Am. Chem. Soc.* **2004**, *126*, 1928–1929.
(51) Andruniow, T.; Kuta, J.; Zgierski, M. Z.; Kozlowski, P. M. *Chem. Phys. Lett.* **2005**, *410*, 410–416.
(52) Kuta, J.; Patchkovskii, S.; Zgierski, M. Z.; Kozlowski, P. M. *J. Comput. Chem.* **2006**, *27*, 1429–1437.
(53) Kozlowski, P. M.; Kuta, J.; Galezowski, W. *J. Phys. Chem. B* **2007**, *111*, 7638–7645.
(54) Rovira, C.; Kozlowski, P. M. *J. Phys. Chem. B* **2007**, *111*, 3251–3257.
(55) Jensen, K. P.; Sauer, S. P. A.; Liljefors, T.; Norrby, P.-O. *Organometallics* **2001**, *20*, 550–556.
(56) Jensen, K. P.; Mikkelsen, K. V. *Inorg. Chim. Acta* **2001**, *323*, 5–15.
(57) Dong, S.; Padmakumar, R.; Banerjee, R.; Spiro, T. G. *J. Am. Chem. Soc.* **1996**, *118*, 9182–9183.
(58) Dong, S.; Padmakumar, R.; Banerjee, R.; Spiro, T. G. *Inorg. Chim. Acta* **1998**, *270*, 392–398.
(59) Kräutler, B.; Konrat, R.; Stupperich, E.; Farber, G.; Gruber, K.; Kratky, C. *Inorg. Chem.* **1994**, *33*, 4128–4139.
(60) Randaccio, L.; Furlan, M.; Geremia, S.; Slouf, M.; Srnova, I.; Toffoli, D. *Inorg. Chem.* **2000**, *39*, 3403–3413.
(61) McCauley, K. M.; Pratt, D. A.; Wilson, S. R.; Shey, J.; Burkey, T. J.; van der Donk, W. *J. Am. Chem. Soc.* **2005**, *127*, 1126–1136.
(62) Wagner, T.; Afshar, C. E.; Carrell, H. L.; Glusker, J. P.; Englert, U.; Hogenkamp, H. P. C. *Inorg. Chem.* **1999**, *38*, 1785–1794.
(63) Pagano, T. G.; Marzilli, L. G.; Flocce, M. M.; Tsai, C.; Carrell, H. L.; Glusker, J. P. *J. Am. Chem. Soc.* **1991**, *113*, 531–542.
(64) Perry, C. B.; Fernandes, M. A.; Marques, H. M. *Acta Crystallogr.* **2004**, *C60*, m165−m167.
(65) Becke, A. D. *J. Chem. Phys.* **1986**, *84*, 4524–4529.
(66) Perdew, J. P. *Phys. Rev. B* **1986**, *33*, 8822–8824.
(67) Frisch, M. J.; Trucks, G. W.; Schlegel, H. B.; Scuseria, G. E.; Robb, M. A.; Cheeseman, J. R.; Montgomery, J., J. A.; Vreven, T.; Kudin, K. N.; Burant, J. C.; Millam, J. M.; Iyengar, S. S.; Tomasi, J.; Barone, V.; Mennucci, B.; Cossi, M.; Scalmani, G.; Rega, N.; Petersson, G. A.; Nakatsuji, H.; Hada, M.; Ehara, M.; Toyota, K.; Fukuda, R.; Hasegawa, J.; Ishida, M.; Nakajima, T.; Honda, Y.; Kitao, O.; Nakai, H.; Klene, M.; Li, X.; Knox, J. E.; Hratchian, H. P.; Cross, J. B.; Bakken, V.; Adamo, C.; Jaramillo, J.; Gomperts, R.; Stratmann, R. E.; Yazyev, O.; Austin, A. J.; Cammi, R.; Pomelli, C.; Ochterski, J. W.; Ayala, P. Y.; Morokuma, K.; Voth, G. A.; Salvador, P.; Dannenberg, J. J.; Zakrzewski, V. G.; Dapprich, S.; Daniels, A. D.; Strain, M. C.; Farkas, O.; Malick, D. K.; Rabuck, A. D.; Raghavachari, K.; Foresman, J. B.; Ortiz, J. V.; Cui, Q.; Baboul, A. G.; Clifford, S.; Cioslowski, J.; Stefanov, B. B.; Liu, G.; Liashenko, A.; Piskorz, P.; Komaromi, I.; Martin, R. L.; Fox, D. J.; Keith, T.; Al-Laham, M. A.; Peng, C. Y.; Nanayakkara, A.; Challacombe, M.; Gill, P. M. W.; Johnson, B.; Chen, W.; Wong, M. W.; Gonzalez, C.; Pople, J. A.; *Gaussian, Inc.*: Wallingford CT, 2004.
(68) Galezowski, W.; Kuta, J.; Kozlowski, P. M. *J. Phys. Chem. B* **2007**, *112*, 3177–3183.
(69) Tested basis sets were: 6-31G(d), 6-311G(d,p), TZVP, and mixed basis sets with combinations of thereof.
(70) Moore, S. J.; Lachicotte, R. J.; Sullivan, S. T.; Marzilli, L. G. *Inorg. Chem.* **1999**, *38*, 383–390.
(71) Randaccio, L.; Geremia, S.; Zangrando, E.; Ebert, C. *Inorg. Chem.* **1994**, *33*, 4641–4650.

JP901397P